The Astronomical Journal, 158:194 (9pp), 2019 November https://doi.org/10.3847/1538-3881/ab46a8

Jupiter's Composition Suggests its Core Assembled Exterior to the N_2 Snowline

Karin I Öberg[1] and Robin Wordsworth[2,3]
[1] Harvard-Smithsonian Center for Astrophysics, 60 Garden St, Cambridge, MA 02138, USA; koberg@cfa.harvard.edu
[2] Harvard Paulson School of Engineering and Applied Sciences, Harvard University, Cambridge, MA 02140, USA
[3] Department of Earth and Planetary Sciences, Harvard University, Cambridge, MA 02140, USA
Received 2019 July 12; revised 2019 September 18; accepted 2019 September 20; published 2019 October 22

Abstract

Jupiter's atmosphere is enriched in C, N, S, P, Ar, Kr, and Xe with respect to solar abundances by a factor of ∼3. Gas giant envelopes are mainly enriched through the dissolution of solids in the atmosphere, and this constant enrichment factor is puzzling since several of the above elements are not expected to have been in the solid phase in Jupiter's feeding zone; most seriously, Ar and the main carrier of N, N_2, only condense at the very low temperatures, 21–26 K, associated with the outer solar nebula. We propose that a plausible solution to the enigma of Jupiter's uniform enrichment pattern is that Jupiter's core formed exterior to the N_2 and Ar snowlines, beyond 30 au, resulting in a solar composition core in all volatiles heavier than Ne. During envelope accretion and planetesimal bombardment, some of the core mixed in with the envelope, causing the observed enrichment pattern. We show that this scenario naturally produces the observed atmosphere composition, even with substantial pollution from N-poor pebble and planetesimal accretion in Jupiter's final feeding zone. We note that giant core formation at large nebular radii is consistent with recent models of gas giant core formation through pebble accretion, which requires the core to form exterior to Jupiter's current location to counter rapid inward migration during the core and envelope formation process. If this scenario is common, gas giant core formation may account for many of the gaps observed in protoplanetary disks between 10 s and 100 au.

Unified Astronomy Thesaurus concepts: Solar system formation (1530); Solar nebulae (1508); Jupiter (873); Planet formation (1241); Protoplanetary disks (1300); Planetary atmospheres (1244); Solar system (1528)

1. Introduction

The compositions of planets are linked to the chemical conditions in the solar nebula. Since chemical conditions change across the nebula, a planet's composition provides clues to its formation locations, and therefore to its dynamical past (Dodson-Robinson et al. 2009; Öberg et al. 2011b; Ciesla et al. 2015). Of all known giant planets, Jupiter presents the most well-constrained composition because of in situ measurements by the *Galileo* and *Juno* missions (Niemann et al. 1996; Bolton et al. 2017). Importantly for this paper, the *Galileo* mission revealed that C, N, S, P, Ar, Kr, and Xe are all enriched with respect to hydrogen compared to solar abundances (Owen et al. 1999). Whether O is enriched is unknown—*Galileo* recorded a subsolar O abundance, but this probably does not reflect the bulk O abundance. Gas giant envelopes can become enriched through a number of processes—core erosion and mixing, accretion of enriched gas, and dissolution of accreting pebbles and planetesimals during envelope accretion or in the subsequent clean-up stage (Hueso & Guillot 2003; Estrada et al. 2017)—and some enrichment compared to solar abundances is therefore not surprising. What is surprising, however, is that all the above species are enriched by approximately the same factor, ∼3.

This enrichment pattern is surprising because the expected solar nebula solid composition at ∼3–5 au, the assumed formation location of Jupiter in most models (e.g., Gomes et al. 2005), is decidedly nonsolar, and most models explain Jupiter's enrichment by solid accretion and dissolution. At 3–5 au, the solids are expected to have been mainly composed of refractory material and water ice (Ciesla et al. 2015), and therefore rich in oxygen (O), sulfur (S), and phosphor (P) (Anders & Grevesse 1989; Asplund et al. 2009), but comparatively poor in carbon (C), and very poor in nitrogen (N) and noble gases (Ar, Kr, and Xe), because important carbon carriers (CO_2 and CO), and the dominant nitrogen carrier (N_2), as well as Xe, Kr, and Ar only freeze out further out in the solar nebula. Accretion of such solids by a gas giant would enrich its envelope strongly in O, S, and P, slightly in C, and not at all in N, Ar, Kr, and Xe, in tension with the observed uniform factor of 3 enrichment in all observed elements.

A possible solution to the presented tension is entrapment of hypervolatiles in water ice, which could maintain more C, and some N, Ar, Kr, and Xe in solids at 5 au. Indeed several models have invoked clathration or entrapment of hypervolatiles in amorphous water ice as explanations of Jupiter's enrichment pattern (Lunine & Stevenson 1985; Owen et al. 1999; Gautier et al. 2001; Hersant et al. 2004; Gautier & Hersant 2005; Mousis et al. 2009). These models face some difficulties, however. First, they require large amounts of water ice to entrap all other volatiles. This should result in an excess enrichment in oxygen by a factor of a few compared to other elements in Jupiter's atmosphere, for which there is so far no evidence. Second, entrapment of CO, N_2, and Ar through clathration requires low nebular temperatures (Lunine & Stevenson 1985; Gautier et al. 2001), 40 K and less, which is difficult to achieve in the nebula at 3–5 au if radiative heating is taken into account.

A possible solution to the difficulty of locally entrapping hypervolatiles at 3–5 au is radial drift of cold pebbles from the outer solar nebula into Jupiter's feeding zone (e.g., Cuzzi & Zahnle 2004; Öberg & Bergin 2016). A similar idea underpins a recent study by Mousis et al. (2019), who consider sublimation of entrapped volatiles in inward-drifting amorphous water-ice pebbles. The enriched gas is then accreted onto Jupiter. While this process likely plays a role, it should not lead to a uniform enhancement in, e.g., N and C. First, even at low temperatures, N_2 entrapment is inefficient compared to CO entrapment

(e.g., Bar-Nun et al. 1985, 2007; Yokochi et al. 2012), which may explain low N_2 abundances in comets (Cochran et al. 2000; Cochran 2002; Rubin et al. 2015). Second, the nebular model must be fine tuned to result in a pebble population at 3–5 au that originates exclusively from the cold, outer solar nebula region, rather than from a range of radii, most of which would not allow for efficient N_2 entrapment.

A simpler explanation to Jupiter's enrichment pattern is that Jupiter's core formed in the outer solar system, beyond the N_2 and Ar snowlines, from solids with solar ratios of all elements heavier than Ne. During envelope accretion and planetesimal and embryo impacts, some of the core was then mixed in with the envelope causing the observed enrichment pattern. Such a formation scenario may appear implausible at first sight, but is supported by both recent theory and observations. First, recent models of core formation through pebble accretion in actively accreting disks only produce a Jupiter-sized planet at Jupiter's location if the core forms substantially further out, at nebular radii >15 au (Bitsch et al. 2015, 2019; Pirani et al. 2019). In earlier generations of gas giant formation models, gas giant formation was limited by long core formation and envelope accretion timescales (e.g., Pollack et al. 1996; Hueso & Guillot 2003), which typically exceeded 5 Myr at 5 au. This is longer than the typical 2–3 Myr lifetime of observed protoplanetary disks (Mamajek 2009), and since timescales increase with nebular radius, gas giant formation in the outer solar nebula seemed excluded. By contrast planet core formation through pebble accretion is fast, and in recent models the whole gas giant formation process—core formation, envelope accretion, and inward migration—can be completed in <1 Myr. Even if core formation begins at ∼40 au the complete process takes only ∼2 Myr (Bitsch et al. 2015).

Second, millimeter observations of analogs to our solar nebula, i.e., of protoplanetary disks, have revealed that gaps appear common at disk radii of 10–100 au (Andrews et al. 2018; Huang et al. 2018). These gaps are proposed to be associated with actively forming planets, and while other explanations exist, there is at least one example where the there is supporting kinematic evidence for protoplanets in the disk gaps (Pinte et al. 2018; Teague et al. 2018). If these gaps are indeed carved out by planets, the gap widths and depths can be used to constrain planet masses; this was recently done for the Disk Substructures at High Angular Resolution Project (DSHARP) disk sample (Andrews et al. 2018; Zhang et al. 2018). The result is that the gaps can be explained by planets and planetary embryos of masses between ∼10 Earth masses and a few Jupiter masses, suggestive of that of a gas giant, or at least gas giant cores often begin their existence at large disk radii.

The pebble accretion scenario has been used in one study to explore whether it can indeed explain Jupiter's composition (Ali-Dib 2017), using a full-scale planet formation and migration model. They found that core formation in the outer solar nebula could not alone account for Jupiter's nitrogen enrichment, probably because of the location of the N_2 snowline in their nebular model. In this paper we take a simpler, toy model approach to explore expected enrichment patterns in Jupiter's envelope when its core forms in the outer regions of the solar nebula, with outer regions defined with respect to the N_2 and Ar snowline locations. Section 2 introduces the nebular snowline model used throughout the paper. In Section 3 we present our fiducial enrichment model and explore how sensitive it is to core and envelope formation locations, as well as to pollution during the clean-up stage. We discuss the results in Section 4 before offering some brief conclusions in Section 5.

2. Solar Nebula Model

2.1. Density and Temperature Structure

To explore the link between Jupiter's core formation location and its observed envelope composition, we construct a simple, static toy model of the radial composition of solids and gas in the solar nebula midplane. We follow the common assumption of radial power laws in surface density and temperature (e.g., Lewis 1974; Chiang & Youdin 2010):

$$\Sigma_{\rm H} = \Sigma_{\rm H,1au}\left(\frac{r}{1\ {\rm au}}\right)^{-\gamma}, \quad (1)$$

$$n_{\rm H} = \frac{\Sigma_{\rm H}}{\sqrt{2\pi}H}, \quad (2)$$

$$H = \frac{k_{\rm b}T}{m_{\rm H}\mu}\sqrt{\frac{r^3}{GM_{\rm Sun}}}, \quad (3)$$

$$T_{\rm mid} = T_{\rm mid,2\ au}\left(\frac{r}{2\ {\rm au}}\right)^{-q}, \quad (4)$$

where $\Sigma_{\rm H}$ is the column density, r is the disk radius in astronomical units, $\Sigma_{\rm H,1\ au}$ is the column density at 1 au, which we set to 1500 g cm^{-2}, and γ is the surface dense power-law index, which is typically assumed to be 3/2 for the solar nebula (Chiang & Youdin 2010). The hydrogen nuclei density $n_{\rm H}$ is calculated from the surface density and the isothermal scale height H. Finally, $T_{\rm mid}$ is the midplane temperature and q is the temperature power-law index. The latter is expected to be ∼3/7 in the outer disk (exterior to a few au), where reprocessed solar radiation dominates disk heating (Chiang & Youdin 2010). However, higher values of up to 0.7 have been inferred from observations (Andrews & Williams 2007).

Rather than adopting theoretical estimates of $T_{\rm mid}$ and q, we use data on solar nebula H_2O, CO, and N_2 snowline locations to set their values. The water snowline has been localized to ∼2 au, though the location likely evolved with time as Jupiter was forming (Min et al. 2011). The CO and N_2 snowlines are more uncertain. Based on comet compositions the CO snowline was likely located in the comet-forming zone, since comets present a large diversity of CO abundances (Mumma & Charnley 2011). This fits with recent estimates of the CO snowline in the TW Hya disk (Zhang et al. 2017). Appreciable amounts of N_2 in comets are rare (Cochran et al. 2000; Cochran 2002; Rubin et al. 2015), though a N_2/CO ratio of 0.15 was recently reported in one comet (Cochran & McKay 2018), and the majority of comets therefore likely formed interior to the N_2 snowline, placing the N_2 snowline in the outer range of the proposed comet-forming region of 5–35 au (Mumma & Charnley 2011). Finally, Pluto appears to be rich in N_2, which would be consistent with formation exterior to the N_2 snowline, though other explanations have been given as well (Stern et al. 2018). Pluto likely formed at 20–30 au (Kenyon & Bromley 2012), and we therefore tune our disk model temperature profile such that the N_2 snowline is at 20–30 au.

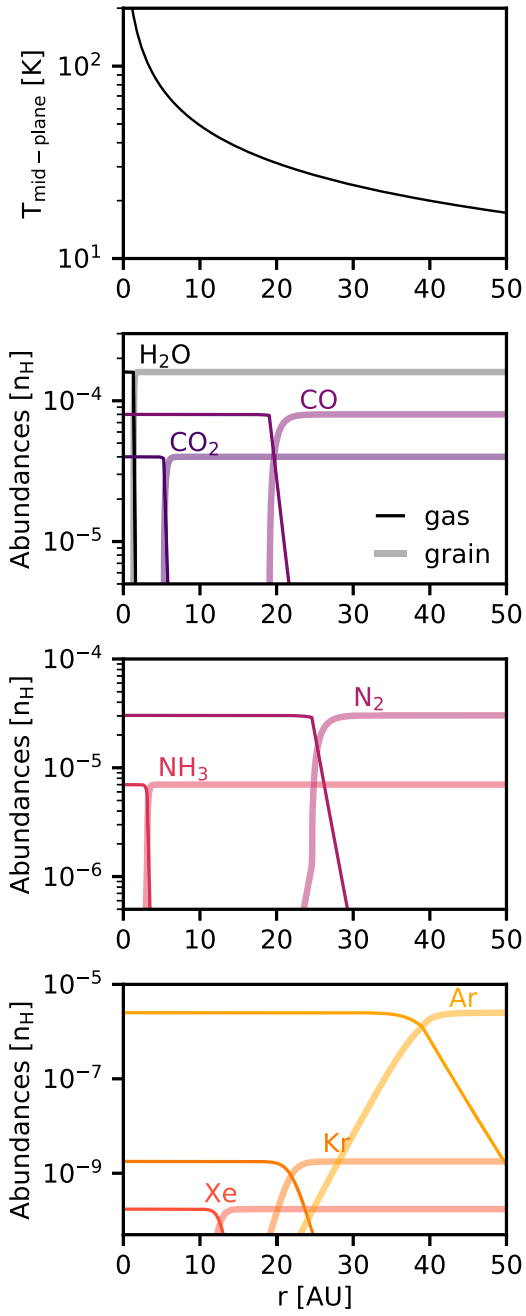

Figure 1. Top: adopted temperature profile for the solar nebula midplane. Lower three panels: Abundances and snowline locations of major carriers of O, C, and N, respectively, as well as of the noble gases assuming no entrapment in less volatile ices.

Using standard values for H_2O, CO, and N_2 sublimation energies of 5800, 1180, and 1051 K, respectively, where the latter two values assume CO and N_2 sublimation from a water-rich ice, we obtain a reasonable fit to the above snowline constraints when $T_{mid,2au} = 140$ K and $q = 0.65$. The resulting temperature profile is shown in the top panel of Figure 1, and the snowline locations of H_2O, CO, and N_2 are plotted in the panels below. We note, however, that a warmer or more shallow temperature profile would have been inferred if pebble drift was included in the model, since pebble drift moves snowlines inward compared to the static case (e.g., Piso et al. 2015). The presented temperature profile should therefore be viewed as a convenient tool to estimate gas and solid abundances across the solar nebula rather than a an accurate model of the solar nebula thermal structure.

Table 1
Adopted Molecular Abundances, Desorption Attempt Frequencies, and Energies

Molecule	Abundance x_i (n_H])	ν_i (s^{-1})	$E_{subl,i}$ (K)
H_2O	1.6×10^{-4}	4×10^{13}	5800[a]
CO_2	4×10^{-5}	1×10^{13}	2700[b]
CO	8×10^{-5}	7×10^{11}	1180[c]
Volatile organics	3×10^{-5}	6×10^{16}	2500[d]
N_2	3×10^{-5}	8×10^{11}	1050[c]
NH_3	7×10^{-6}	1×10^{13}	3800[e]
Ar	2.5×10^{-6}	6×10^{11}	870[f,g]
Kr	1.8×10^{-9}	1.2×10^{14}	1380[f]
Xe	1.7×10^{-10}	4.6×10^{14}	1970[f]

Notes.
[a] Fraser et al. (2001).
[b] Sandford & Allamandola (1990).
[c] Fayolle et al. (2016).
[d] Behmard et al. (2019).
[e] Suhasaria et al. (2015).
[f] Smith et al. (2016), using their binding energies to compact water.

2.2. Molecular Abundances and Snowline Locations

The gas and solid-state distributions of elements in a disk are primarily set by the condensation lines of major element carriers, e.g., silicate grains, H_2O CO, and CO_2 for oxygen. In this paper we consider only the elements that have been quantified in Jupiter's atmosphere, i.e., O, C, N, P, S, Xe, Kr, and Ar. The carriers of several of these are unfortunately poorly constrained and the estimates in Table 1 should be treated as provisional. Our general strategy is to use data from the interstellar medium (ISM), which provides abundance baselines for the young solar nebula, and augment with solar system data as available.

In the dense ISM, oxygen is mainly carried by silicate grains, H_2O, CO, and CO_2, with similar amounts of O in the first three carriers, while CO_2 is present at a ~25% level compared to water (Whittet 2010; Öberg et al. 2011a; Boogert et al. 2015). In comets, H_2O appears more abundant than silicate, while CO_2 is ~20% compared to water and CO abundances vary (Mumma & Charnley 2011). We adopt a mixed scheme with equal abundances of O in H_2O and silicate grains, and CO and CO_2 abundances that are 50% and 25% compared to H_2O, respectively, and set the absolute abundances so that they add up to solar (Asplund et al. 2009).

Based on the oxygen budget above, 50% of the carbon is in CO and CO_2. We split the remaining carbon into one part volatile organics, using ethane as a model system, and three parts carbon grains and refractory organics. For nitrogen, ISM data shows that ~10% of nitrogen is in NH_3, while solar system, ISM, and protoplanetary disk data alike indicate that most of the remaining (~90%) nitrogen is in N_2 (Öberg et al. 2011a; Pontoppidan & Blevins 2014), and we use these estimates. Both S and P are heavily depleted in the ISM, indicative of refractory carriers. Finally the noble gases are assumed to be present in atomic form. All abundances are listed in Table 1.

We assume silicate grains, carbon grains, and refractory organics, S and P, which are all present in the solid state at all

relevant radii. The abundances of all other species are modeled to solely depend on the changing balance between sublimation and condensation as a function of radius. Condensation rates are described by

$$R_{\mathrm{cond},i} = n_{\mathrm{gr}} n_{i,\mathrm{gas}} v_i \sigma_{\mathrm{gr}}, \quad (5)$$

where n_{gr} is the grain number density, $n_{i,\mathrm{gas}}$ the number density of species i in the gas-phase, v_i the collisional velocity of grains and species i which is assumed to the be the thermal velocity of i, and σ_{gr} is the collisional cross-section which is the cross-section of the grain. It is useful to rewrite this equation in terms of abundances x with respect to the main constituent of the solar nebula, hydrogen nuclei, in which case the equation instead becomes

$$R_{\mathrm{cond},i} = x_{\mathrm{gr}} x_{i,\mathrm{gas}} n_{\mathrm{H}}^2 v_i \sigma_{\mathrm{gr}}. \quad (6)$$

Sublimation is described in detail by, e.g., Fraser et al. (2001) and Bisschop et al. (2006). In summary, for low surface coverages where all surface molecules are available for sublimation, sublimation is calculated from

$$R_{\mathrm{subl},i} = x_{i,\mathrm{grain}} n_{\mathrm{H}} \times \nu_i \,\mathrm{Exp}(E_{\mathrm{subl},i}/T), \quad (7)$$

where $x_{i,\mathrm{grain}}$ is the abundance of i frozen out on grains, ν_{i} is the attempt frequency, $E_{\mathrm{subl},i}$ is the sublimation barrier in units of Kelvin, and T is the grain temperature which is assumed to be perfectly coupled to the gas temperature in the dense disk midplane. Sublimation energies and attempt frequencies for all species are listed in Table 1. For higher surface coverages, where only the top layer of the ice can sublime, the sublimation rate is instead

$$R_{\mathrm{subl},i} = x_{\mathrm{grain}} n_{\mathrm{H}} 10^{15} 4 \sigma_{\mathrm{grain}} \times \nu_i \,\mathrm{Exp}(E_{\mathrm{subl},i}/T). \quad (8)$$

We assume that there is a steady state between sublimation and condensation at each radius, and that the total abundance $x_i = x_{i,\mathrm{gas}} + x_{i,\mathrm{gr}}$ is constant. We then use the adopted disk temperature and midplane hydrogen density profile to calculate the gas and grain abundance of each species as a function of solar nebula radius. The results of these calculations are shown in Figure 1. Note that the CO snowline is at ~20 au and the N_2 snowline is at ~26 au, in agreement with the above snowline location constraints from solar system composition data. The Ar snowline at ~40 au is the most distant one in our model; under nebular conditions and using the binding to water ice reported by Smith et al. (2016), Ar only freezes out <21 K. More recent, unpublished data suggests a slightly higher Ar condensation temperature of ~25 K (T. Schneiderman, private communication), which would move the Ar snowline close to the N_2 snowline. We use the published value in this study, but note that the existing Ar sublimation data may place Jupiter's inception 10 au further out than is actually required.

3. Results

3.1. Nebular Elemental Solid Ratios

We can use the snowline calculations above to calculate the relative abundances of O, C, N, P, S, Ar, Kr, and Xe in solids, and hence the achievable enrichment patterns for a planet forming at different radii. Figure 2 shows the O, C, and N solid abundances with respect to S, normalized to solar abundances. Sulfur is a reasonable reference element since it is a solid at all relevant radii. At 5 au, the solid-state O/S, C/S, and N/S ratios are 0.76, 0.41, and 0.10, respectively. This entails that an atmosphere enriched with solids at this radii, i.e., the current location of Jupiter, will not obtain a close-to-uniform enrichment pattern unless entrapment of N_2 and noble gases is extremely efficient. O/S, C/S, and N/S solid-state ratios approach solar as the distance from the Sun increases, and become solar beyond the N_2 snowline at 26 au. Beyond 40 au, even Ar freezes out resulting in icy solids with solar composition except for in H, He, and Ne.

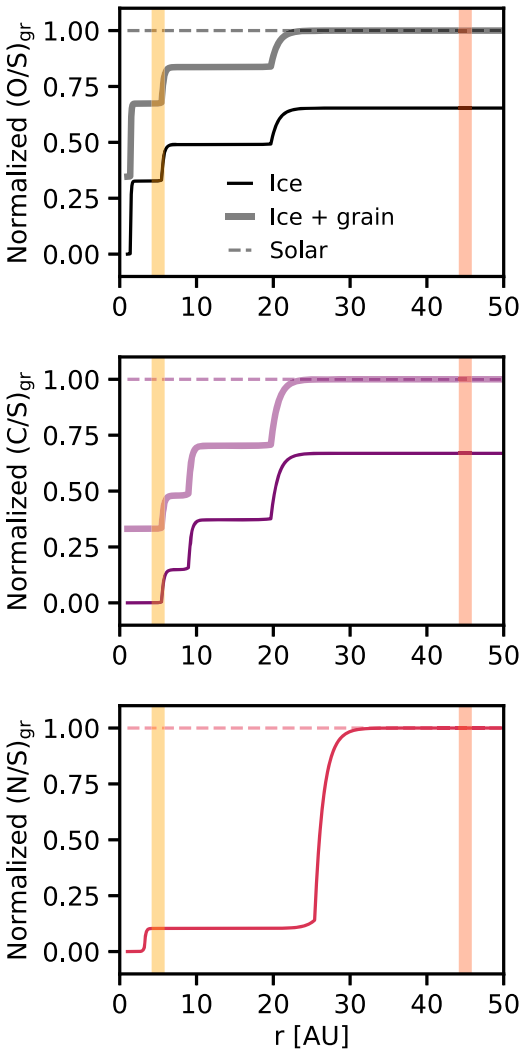

Figure 2. Expected abundance ratios between O, C, N, and S in the solar nebula normalized to solar. Thin lines account for ices, and thick lines for ices and refractory grain material. The transparent light orange band marks the current location of Jupiter at 5 au and the transparent dark orange band marks the location of its core formation at 45 au in our fiducial model, though core formation at 30 au would be sufficient to account to Jupiter's N enrichment. Note that without substantial entrapment in water ice the C/S and N/S ratios in solids are low around Jupiter's current location.

3.2. Fiducial Model for Jupiter's Formation

Considering (1) that solids are only expected to have solar composition in O, C, N, S, P, and noble gases in the outer solar nebula, and (2) that Jupiter appears uniformly enriched in these same elements, it follows that Jupiter likely formed with substantial amounts of outer nebula solids. To account for this, our fiducial model assumes that Jupiter's core formed beyond 45 au, and thus contains a large reservoir of heavy elements at

solar ratios. Based on, e.g., Bitsch et al. (2015), we further assume that the newly formed core migrated inwards toward its current location, while it accreted most of its envelope—the estimated formation+migration timescale from 45 au is ~2.5 Myr (Bitsch et al. 2015). For simplicity we assume that the majority of the envelope was accreted close to 5 au and thus has a 5 au gas composition. Over time this envelope became enriched by dissolution and outward mixing of the core (dredging; Stevenson 1982; Wahl et al. 2017), and by local (5 au) accretion of solids which dissolved in the gaseous envelope.

The model hinges on the possibility of dissolution of both the core and later accreted solids. Models of impacts of ice-rich planetesimals with radii of 30 m–1 km show complete ablation in the outer envelope for a wide range of parameters (Pollack et al. 1996; Iaroslavitz & Podolak 2007). More refractory planetesimals and larger objects show more mixed behavior (Pinhas et al. 2016). To our knowledge there is no similar calculation for pebbles, but it is commonly assumed that icy pebbles completely dissolve, while refractory pebbles may or may not reach the core (Venturini et al. 2016). For simplicity, we assume complete dissolution of impacting pebbles and planetesimals in the gaseous envelope, but this may require an update as more calculations become available. The main effect on our model, if refractory material does not dissolve, would be to lower the P and S enhancements originating from impacting pebbles and planetesimals. The efficiency of core mixing is even more uncertain and we discuss it further in Section 4.

The relative contributions of core mixing and dissolution of locally accreted solids to Jupiter's atmosphere are unknown. In our fiducial model we scale their relative contributions, such that half of the sulfur in Jupiter's envelope, our reference species, originates from core mixing and half from solid accretion at 5 au. This 50–50 divide is somewhat arbitrary and simply encodes a scenario where there are substantial contributions from both reservoirs (in the next section we explore scenarios where one or the other dominates). We scale the total core and local enrichment such that the sulfur enrichment in Jupiter's envelope agrees with observations. The resulting elemental composition in Jupiter's atmosphere can then be traced back to three different sources: mixing of the core, which results in a constant enhancement of all species; accretion of gas at 5 au, which is subsolar in O, S, and P, and almost solar in all other elements; and accretion of solids at 5 au, which are rich in O, S, and P, contain some C, little N, and no noble gases.

Figure 3 shows the resulting enrichment pattern. The model agrees with all measured abundances, except for oxygen, but the *Galileo* measurement of oxygen is generally assumed to not be representative of Jupiter's true composition. For all elements, core mixing provides at least 50% of the measured envelope abundances given our model assumptions, while local solid and gas accretion provides the remainder; gas accretion is more important for C, N, and noble gases, while local solid accretion accounts for the remainder of O, S, and P.

3.3. Model Grid Results

To evaluate the sensitivity of our results to the formation and migration history of Jupiter, Figure 4 explores the outcomes of different combinations of core formation locations, gas envelope accretion locations, and relative contributions from core mixing and planetesimal dissolution on the predicted

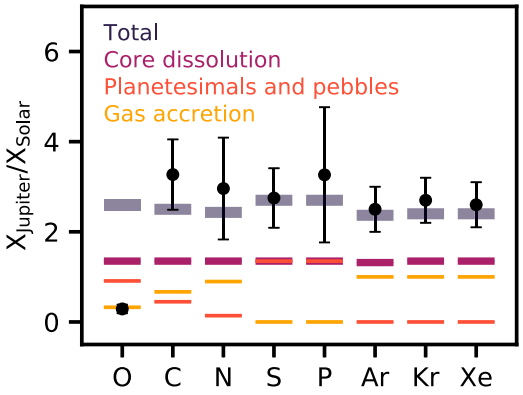

Figure 3. Expected elemental enhancement ratios in Jupiter's envelope in our fiducial model compared to solar (thick blue lines) and the contributions from core mixing, planetesimal dissolution, and gas envelope accretion. Black points are measurements from *Galileo* (O, C, S, Ar, Kr, and Xe; Mahaffy et al. 2000; Wong et al. 2004), *Cassini* (P; Fletcher et al. 2009), and *Juno* (N; Bolton et al. 2017)).

element enhancements in Jupiter's envelope. Similarly to the fiducial model, we fix the total amount of solid dissolution such that the sulphur enhancement matches the observed one.

In the first set of models (left column), the core and gas are accreted at the same location between 45 and 5 au, and all enhancements can be traced back to the solid and gas compositions at the initial formation location. This is a toy version of a scenario where initial migration is slow. In this scenario, formation at 45 au is consistent with data because all elements in question are at equal abundances exterior to the Ar snowline. Complete formation at 30 au also provides a good fit to the data with the exception of Ar, which, as mentioned above, may in reality condense further in than this model suggests. Formation at smaller radii provides a poor fit, because of the low solid abundance of N, Ar, and Kr at 15 au, and of N, C, Ar, Kr, and Xe at 5 au, which entails that they are predicted to be present in Jupiter's atmosphere at solar levels, rather than the ~2 times higher levels observed. While complete planet formation beyond 30 au is consistent with Jupiter's abundance pattern, we note that it is not supported by either theory (e.g., Bitsch et al. 2015) or by observations (e.g., Kruijer et al. 2017) and are only presented here as model end members.

In the second column of Figure 4 we consider models where the solids originate in the outer solar system, while the gas envelope is accreted at 15 or 5 au. This mimics scenarios where the core forms early at 15–45 au, and the envelope is accreted during inward migration closer to Jupiter's present-day location and later planetesimal accretion and dissolution is inefficient. None of the models result in perfect fits to observations. The models where the core forms at 30–45 au provide good fits to C, N, S, and P, but not to the noble gases, which are either under- or overpredicted, while core formation at 15 au also fails to reproduce N.

The third and last column of Figure 4 explores elemental enhancements in Jupiter's envelope when a fraction of the dissolved solids polluting the envelope originates from a core formed at 45 au and the remainder from solid accretion at 5 au. This assumes the same scenario as in the fiducial model and simply varies the relative contributions from the core and later accreted pebbles, boulders, and planetesimals. We consider scenarios where core mixing contributes 90%, 70%, 50%, and 30% of the total solids dissolved in Jupiter's envelope, and as Figure 4 shows, the two intermediate cases provide good

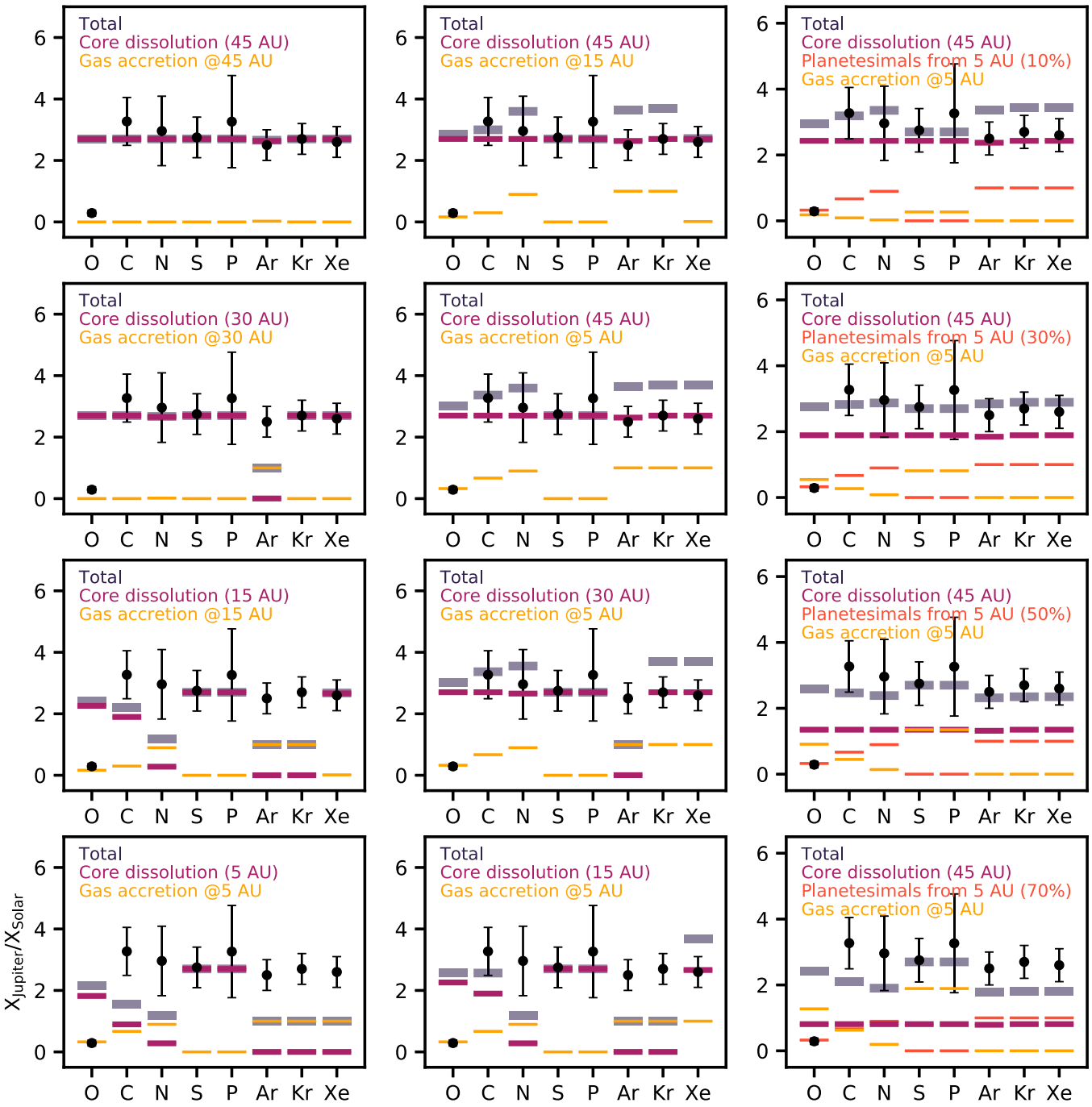

Figure 4. Same as Figure 3, but for different combinations of solid and gas accretion locations. Left: predicted elemental enhancements in Jupiter's envelope when solids and envelope are accreted at the same disk radius. Middle: predicted elemental enhancements when the gas is accreted interior to the core formation location. Right: predicted enhancements when a fraction of the solids dissolved in the envelope originates from a core formed at 45 au and a fraction from planetesimals accreted at 5 au. Note that only scenarios where Jupiter's core forms at 45 au fit all of the data. If Ar condenses out closer to the N_2 snowline, as suggested by recent unpublished data, core formation beyond 30 au is sufficient to explain observations.

fits to observations, while the two extremes deviate from observations.

In summary, Jupiter's composition is only well reproduced if it obtained a large amount of solids from the outer solar system through core formation exterior to the N_2 and Ar snowlines, which in our disk model are placed at ~26 and 40 au, respectively. Though note that the latter may became revised inwards with new laboratory data made available (T. Schneiderman 2019, private communication). Once the core is formed, it is possible to reproduce all observed abundances if Jupiter either accreted its gaseous envelope in the outer solar system or if it accreted its envelope at smaller radii together with a substantial amount of dissolvable solids in the form of pebbles and planetesimals.

4. Discussion

4.1. Core Formation and Mixing

We have showed that formation of Jupiter's core exterior to the N_2 and Ar snowlines, followed by core mixing into the gaseous envelope, provides a good fit to Jupiter volatile

abundances when combined with inward migration, and with gas and further pebble and planetesimal accretion in the inner solar nebula. This model hinges on several assumptions, (1) that it is possible to form a large, ∼20 Earth mass planetary core in the outer solar nebula, (2) that it can migrate to Jupiter's current location before the nebular gas dissipates, and (3) that a substantial portion of that core, >50%, could become dissolved in Jupiter's envelope. The plausibilities of these processes are the subjects of this subsection.

As introduced in Section 1, pebble accretion models that include a full dynamical treatment of the disk and nascent planets predict that Jupiter's core formed substantially further out in the solar system compared to Jupiter's present location (Bitsch et al. 2015; Ali-Dib 2017; Bitsch et al. 2019). How far out in the disk depends on when the core formed and on the disk mass and metallicity. The latter two are poorly constrained from solar system data and protoplanetary disk studies alike. Observations of protoplanetary disks may provide some information about when planet formation typically begins, however, assuming that observed substructures are associated with planet formation. The youngest disks that show substantial gaps are <1 Myr old, including the iconic HL Tau disk (ALMA Partnership et al. 2015). This suggests that the onset planet core formation is <1 Myr as well. Bitsch et al. (2015) showed that the earlier Jupiter's core formed, the further out in the disk it must have originated—if it formed within a 1 Myr of the inception of the solar nebula and the nebula lasted for 3 Myr, Jupiter's core likely formed beyond 30 au, in agreement with our model requirements.

If Jupiter's core formed in the outer solar system, could it also have accreted its envelope at >30 au? Recent analyses of asteroid population data suggests that Jupiter's core was in place early in the history of the solar system (Kruijer et al. 2017). This favors a scenario where the core alone formed at large distances and then migrated inwards. Recent work by Pirani et al. (2019) also places Jupiter's core formation in the outer solar system, based on Trojan data, while most of the gas envelope is accreted closer to 5 au, consistent with our fiducial model.

The next issue is whether nitrogen and other elements accumulated during core formation would remain trapped in the core, or become well mixed throughout Jupiter's interior after the planet's gas envelope was captured. Previous ab initio calculations have shown that elements as heavy as Fe and Mg should be soluble in hydrogen at the pressures and temperatures expected in Jupiter's interior (Wilson & Militzer 2012b; Wahl et al. 2013; González-Cataldo et al. 2014). Water ice is soluble at temperatures of around 3000 K at Jovian interior pressures (Wilson & Militzer 2012a), which is much lower than the temperatures expected in the region of Jupiter's core. An initially icy core accreted in the outer solar system should therefore dissolve into the nearby hydrogen envelope.

Although dissolution of heavy species from a core into a pure hydrogen envelope is expected, subsequent mixing into the gas envelope depends on convective processes that are still poorly understood under Jovian conditions (Leconte & Chabrier 2013; Nettelmann et al. 2015; Moll et al. 2017). Double-diffusive layered convection, if present, could reduce mixing efficiency, although its importance throughout Jupiter's evolutionary history is debated (Leconte & Chabrier 2013; Moll et al. 2017; Vazan et al. 2018). While the theory remains to be worked out there is recent empirical support for a core dissolution and dredging scenario: inter-comparison of interior models with Jupiter's low-order gravitational moments J_2–J_8 measured by *Juno* suggests a large, dilute core, which is consistent with a significant amount of core dredging having occurred (Wahl et al. 2017). To account for this Liu et al. (2019) proposed that the young Jupiter collided head-on with a large planet embryo, which shattered Jupiter's primordial core, and distributed its heavy elements into the inner envelope.

4.2. The Role of Volatile Entrapment

So far all our models have assumed that volatile entrapment was unimportant in setting the bulk elemental abundances in the solar system. This is opposite to most previous explanations of Jupiter's enrichment pattern. We therefore briefly explore the outcome of our model when incorporating maximum entrapment assuming that ∼5 H_2O molecules are required for each entrapped hypervolatile, a 100% entrapment efficiency, and that the hypervolatiles under consideration, CO, N_2, and noble gases, are all entrapped equally well. In other words we assume that an equal proportion of each hypervolatile is entrapped such that their sum does not exceed 20% of the total number of water molecules. This likely overpredicts the amount of possible N_2 entrapment, since experiments show that N_2 is less efficiently trapped than CO (e.g., Bar-Nun et al. 1985, 2007; Yokochi et al. 2012), and thus provides a limiting case for testing our conclusions. The assumption of that at least five water molecules are needed for each entrapped hypervolatile is based on both clathration (Lunine & Stevenson 1985) and amorphous ice entrapment studies (Notesco et al. 2003; Fayolle et al. 2011; Simon et al. 2019).

Based on the adopted water and hypervolatile abundances, a maximum of 28% of the nebular hypervolatiles can become trapped. Figure 5 shows the results when incorporating this maximum level of entrapment for the fiducial model, and for a model where Jupiter completely forms at 5 au. The fiducial model results are basically unchanged by including entrapment. By contrast, in the model where Jupiter forms in situ, including entrapment does enhance N, C, and noble gas abundances, but even our very optimistic, maximum entrapment assumption does not result in sufficient CO, N_2, or noble gases to explain the observations. It is important to note that it is quite difficult to conceive of a scenario where maximum entrapment would occur, since N_2 is likely to freeze out on top of the H_2O ice matrix in the cooling nebula rather than becoming perfectly mixed in with it, and should be trapped with a lower efficiency than the more abundant CO.

4.3. Predictions for Outer Solar System Missions

The strongest prediction emerging from our model is that the oxygen enhancement in Jupiter should be similar to that of C and N, i.e., that it is not substantially more enhanced. This is distinct from models that require entrapment of C and N carriers in H_2O ice, where oxygen will be enhanced by a substantially higher factor.

A second set of predictions concerns Saturn. If Saturn and Jupiter formed at the same time, Saturn's inception was likely ∼3 au exterior to Jupiter's (Pirani et al. 2019). In our model that places Saturn's formation well outside of the N_2 and Ar snowlines, and we should expect a similar enrichment pattern in Saturn as in Jupiter, i.e., a near constant enrichment of O, C, N, S, P, Xe, Kr, and Ar in Saturn's envelope. The

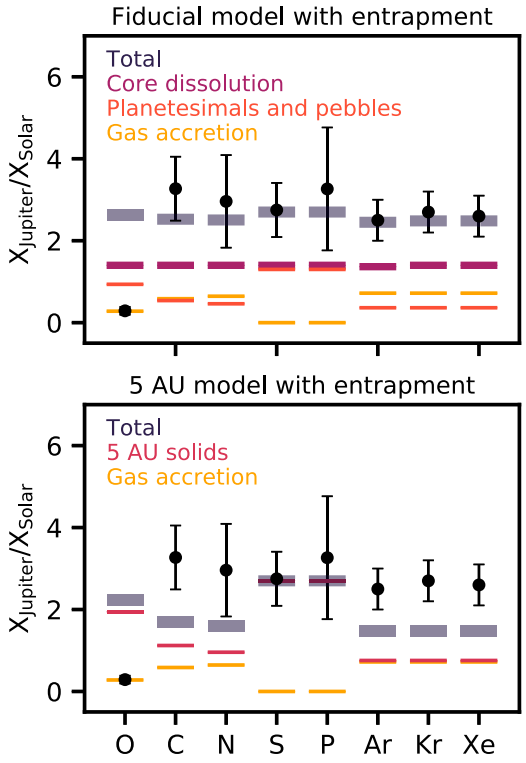

Figure 5. Jupiter envelope element enhancements over solar in our fiducial model and in a model where Jupiter's core and envelope accrete at 5 au, assuming maximum entrapment of CO, N_2, and noble gases in water ice.

formation timescale for both Saturn and Jupiter would be 2–3 Myr and they would therefore have to start forming when the solar nebula was <1 Myr old (Bitsch et al. 2015). Another possible scenario is that Saturn formed after Jupiter had already fully assembled and migrated to its final position. In this scenario Saturn's core would begin to form when the solar nebula was already older than 2 Myr, since it takes ~2 Myr for a Jupiter-sized planet to form and migrate into place if its inception is beyond 30 au. Adopting a disk lifetime of 3 Myr, Saturn would then need to form in <1 Myr, which limits its formation location to 15–20 au according to the model grid presented in Bitsch et al. (2015). In this scenario, P, O, C, Xe, and Kr should all be similarly enhanced in Saturn's envelope, while N and Ar should be underabundant. Better constraints on Saturn's elemental composition is thus key to constrain when and how the outer solar system assembled.

5. Conclusions

Jupiter's near-uniform enhancements in C, N, S, P, Ar, Kr, and Xe are difficult to explain if Jupiter formed close to its current location at 5 au from the Sun. At these radii solids are expected to be depleted in nitrogen, carbon, and noble gases compared to oxygen, sulphur, and phosphorous, and Jupiter's composition cannot then be explained by the accretion of locally assembled solids. Transport of solids from the outer solar system might provide a partial answer, but to fit observations N_2 entrapment in water ice would have to be near complete in the outer solar nebula, and locally assembled pebbles and planetesimals must have been prevented from polluting Jupiter's envelope with O-rich solids. Both seem unlikely, but a final test will come with *Juno*'s measurement of oxygen in Jupiter's envelope. If the observed nitrogen enhancement is due to N_2 entrapment in water, the oxygen enrichment in Jupiter should be high, since at least five, and more likely 10, water molecules are required for each entrapped N_2 molecule.

We propose that Jupiter's abundances are instead due to that Jupiter's core formed in the cold (<25 K), outer solar nebula, beyond the N_2 and Ar snowlines. At these radii (>30 au) solids contained solar ratios between O, C, N, S, P, and noble gases. During envelope accretion and later planetesimal bombardment, a substantial fraction of the primordial core was dissolved into Jupiter's envelope, producing the characteristic abundance pattern. Based on a small set of toy models, this scenario is robust to later solid accretion close to Jupiter's current feeding zone during, e.g., the clean-up phase of planet formation, as long as a majority of solids dissolved in Jupiter's envelope originated beyond the N_2 and Ar snowlines. A key prediction of this model is that oxygen should be enhanced at a similar level to carbon and nitrogen in Jupiter's envelope.

We note that our proposed formation location for Jupiter's core is consistent with recent pebble accretion models, which also place Jupiter's inception in the outer solar nebula, and with observations of an extended core in Jupiter. It also fits with increasing evidence of planet-induced substructure at 10 s of astronomical units in many protoplanetary disks, suggesting that gas giants may commonly begin their existence at 10 s of au, followed by inward migration during their early stages of formation.

K.I.Ö. acknowledges support from the Packard Foundation and R.W. acknowledges support from NASA Habitable Worlds grant NNX16AR86G.

ORCID iDs

Karin I Öberg https://orcid.org/0000-0001-8798-1347

References

Ali-Dib, M. 2017, MNRAS, 464, 4282
ALMA Partnership, Brogan, C. L., Pérez, L. M., et al. 2015, ApJL, 808, L3
Anders, E., & Grevesse, N. 1989, GeCoA, 53, 197
Andrews, S. M., Huang, J., Pérez, L. M., et al. 2018, ApJL, 869, L41
Andrews, S. M., & Williams, J. P. 2007, ApJ, 659, 705
Asplund, M., Grevesse, N., Sauval, A. J., & Scott, P. 2009, ARA&A, 47, 481
Bar-Nun, A., Herman, G., Laufer, D., & Rappaport, M. L. 1985, Icar, 63, 317
Bar-Nun, A., Notesco, G., & Owen, T. 2007, Icar, 190, 655
Behmard, A., Fayolle, E. C., Graninger, D. M., et al. 2019, ApJ, 875, 73
Bisschop, S. E., Fraser, H. J., Öberg, K. I., van Dishoeck, E. F., & Schlemmer, S. 2006, A&A, 449, 1297
Bitsch, B., Izidoro, A., Johansen, A., et al. 2019, A&A, 623, A88
Bitsch, B., Lambrechts, M., & Johansen, A. 2015, A&A, 582, A112
Bolton, S. J., Adriani, A., Adumitroaie, V., et al. 2017, Sci, 356, 821
Boogert, A. C. A., Gerakines, P. A., & Whittet, D. C. B. 2015, ARA&A, 53, 541
Chiang, E., & Youdin, A. N. 2010, AREPS, 38, 493
Ciesla, F. J., Mulders, G. D., Pascucci, I., & Apai, D. 2015, ApJ, 804, 9
Cochran, A. L. 2002, ApJL, 576, L165
Cochran, A. L., Cochran, W. D., & Barker, E. S. 2000, Icar, 146, 583
Cochran, A. L., & McKay, A. J. 2018, ApJL, 854, L10
Cuzzi, J. N., & Zahnle, K. J. 2004, ApJ, 614, 490
Dodson-Robinson, S. E., Willacy, K., Bodenheimer, P., Turner, N. J., & Beichman, C. A. 2009, Icar, 200, 672
Estrada, P., Mosqueira, I., Lissauer, J., D'Angelo, G., & Cruikshank, D. 2017, in Europa, ed. R. T. Pappalardo, W. B. McKinnon, & K. Khurana (Tucson, AZ: Univ. Arizona Press), 27
Fayolle, E. C., Balfe, J., Loomis, R., et al. 2016, ApJL, 816, L28
Fayolle, E. C., Bertin, M., Romanzin, C., et al. 2011, ApJL, 739, L36
Fletcher, L. N., Orton, G. S., Teanby, N. A., & Irwin, P. G. J. 2009, Icar, 202, 543

Fraser, H. J., Collings, M. P., McCoustra, M. R. S., & Williams, D. A. 2001, MNRAS, 327, 1165
Gautier, D., & Hersant, F. 2005, SSRv, 116, 25
Gautier, D., Hersant, F., Mousis, O., & Lunine, J. I. 2001, ApJL, 550, L227
Gomes, R., Levison, H. F., Tsiganis, K., & Morbidelli, A. 2005, Natur, 435, 466
González-Cataldo, F., Wilson, H. F., & Militzer, B. 2014, ApJ, 787, 79
Hersant, F., Gautier, D., & Lunine, J. I. 2004, P&SS, 52, 623
Huang, J., Andrews, S. M., Dullemond, C. P., et al. 2018, ApJL, 869, L42
Hueso, R., & Guillot, T. 2003, SSRv, 106, 105
Iaroslavitz, E., & Podolak, M. 2007, Icar, 187, 600
Kenyon, S. J., & Bromley, B. C. 2012, AJ, 143, 63
Kruijer, T. S., Burkhardt, C., Budde, G., & Kleine, T. 2017, PNAS, 114, 6712
Leconte, J., & Chabrier, G. 2013, NatGe, 6, 347
Lewis, J. S. 1974, Sci, 186, 440
Liu, S.-F., Hori, Y., Müller, S., et al. 2019, Natur, 572, 355
Lunine, J. I., & Stevenson, D. J. 1985, ApJS, 58, 493
Mahaffy, P. R., Niemann, H. B., Alpert, A., et al. 2000, JGR, 105, 15061
Mamajek, E. E. 2009, in AIP Conf. Ser. 1158, Exoplanets and Disks: Their Formation and Diversity, ed. T. Usuda, M. Tamura, & M. Ishii (Melville, NY: AIP), 3
Min, M., Dullemond, C. P., Kama, M., & Dominik, C. 2011, Icar, 212, 416
Moll, R., Garaud, P., Mankovich, C., & Fortney, J. 2017, ApJ, 849, 24
Mousis, O., Marboeuf, U., Lunine, J. I., et al. 2009, ApJ, 696, 1348
Mousis, O., Ronnet, T., & Lunine, J. I. 2019, ApJ, 875, 9
Mumma, M. J., & Charnley, S. B. 2011, ARA&A, 49, 471
Nettelmann, N., Fortney, J., Moore, K., & Mankovich, C. 2015, MNRAS, 447, 3422
Niemann, H. B., Atreya, S. K., Carignan, G. R., et al. 1996, Sci, 272, 846
Notesco, G., Bar-Nun, A., & Owen, T. 2003, Icar, 162, 183
Öberg, K. I., & Bergin, E. A. 2016, ApJL, 831, L19
Öberg, K. I., Boogert, A. C. A., Pontoppidan, K. M., et al. 2011a, ApJ, 740, 109
Öberg, K. I., Qi, C., Wilner, D. J., & Andrews, S. M. 2011b, ApJ, 743, 152
Owen, T., Mahaffy, P., Niemann, H. B., et al. 1999, Natur, 402, 269
Pinhas, A., Madhusudhan, N., & Clarke, C. 2016, MNRAS, 463, 4516
Pinte, C., Price, D. J., Ménard, F., et al. 2018, ApJL, 860, L13
Pirani, S., Johansen, A., Bitsch, B., Mustill, A. J., & Turrini, D. 2019, A&A, 623, A169
Piso, A.-M. A., Öberg, K. I., Birnstiel, T., & Murray-Clay, R. A. 2015, ApJ, 815, 109
Pollack, J. B., Hubickyj, O., Bodenheimer, P., et al. 1996, Icar, 124, 62
Pontoppidan, K. M., & Blevins, S. M. 2014, FaDi, 169, 49
Rubin, M., Altwegg, K., Balsiger, H., et al. 2015, Sci, 348, 232
Sandford, S. A., & Allamandola, L. J. 1990, ApJ, 355, 357
Simon, A., Oberg, K. I., Rajappan, M., & Maksiutenko, P. 2019, ApJ, 883, 21
Smith, R. S., May, R. A., & Kay, B. D. 2016, JPCB, 120, 1979
Stern, S. A., Grundy, W. M., McKinnon, W. B., Weaver, H. A., & Young, L. A. 2018, ARA&A, 56, 357
Stevenson, D. J. 1982, P&SS, 30, 755
Suhasaria, T., Thrower, J. D., & Zacharias, H. 2015, MNRAS, 454, 3317
Teague, R., Bae, J., Bergin, E. A., Birnstiel, T., & Foreman-Mackey, D. 2018, ApJL, 860, L12
Vazan, A., Helled, R., & Guillot, T. 2018, A&A, 610, L14
Venturini, J., Alibert, Y., & Benz, W. 2016, A&A, 596, A90
Wahl, S. M., Hubbard, W. B., Militzer, B., et al. 2017, GeoRL, 44, 4649
Wahl, S. M., Wilson, H. F., & Militzer, B. 2013, ApJ, 773, 95
Whittet, D. C. B. 2010, ApJ, 710, 1009
Wilson, H., & Militzer, B. 2012a, ApJ, 745, 54
Wilson, H. F., & Militzer, B. 2012b, PhRvL, 108, 111101
Wong, M. H., Mahaffy, P. R., Atreya, S. K., Niemann, H. B., & Owen, T. C. 2004, Icar, 171, 153
Yokochi, R., Marboeuf, U., Quirico, E., & Schmitt, B. 2012, Icar, 218, 760
Zhang, K., Bergin, E. A., Blake, G. A., Cleeves, L. I., & Schwarz, K. R. 2017, NatAs, 1, 0130
Zhang, S., Zhu, Z., Huang, J., et al. 2018, ApJL, 869, L47

The Astronomical Journal, 159:78 (1pp), 2020 February https://doi.org/10.3847/1538-3881/ab6172

Erratum: "Jupiter's Composition Suggests Its Core Assembled Exterior to the N_2 Snowline" (2019, AJ, 158, 194)

Karin I Öberg[1] and Robin Wordsworth[2,3]
[1] Harvard-Smithsonian Center for Astrophysics, 60 Garden Street, Cambridge, MA 02138, USA; koberg@cfa.harvard.edu
[2] Harvard Paulson School of Engineering and Applied Sciences, Harvard University, Cambridge, MA 02140, USA
[3] Department of Earth and Planetary Sciences, Harvard University, Cambridge, MA 02140, USA
Received 2019 December 10; published 2020 January 31

In the published article, there was a mismatch between the legend and line colors for the gas and planetesimal accretion contributions to Jupiter's O, C, N , S, P, Ar, Kr, and Xe abundances in the right panels of Figure 4. The correct figure is shown below.

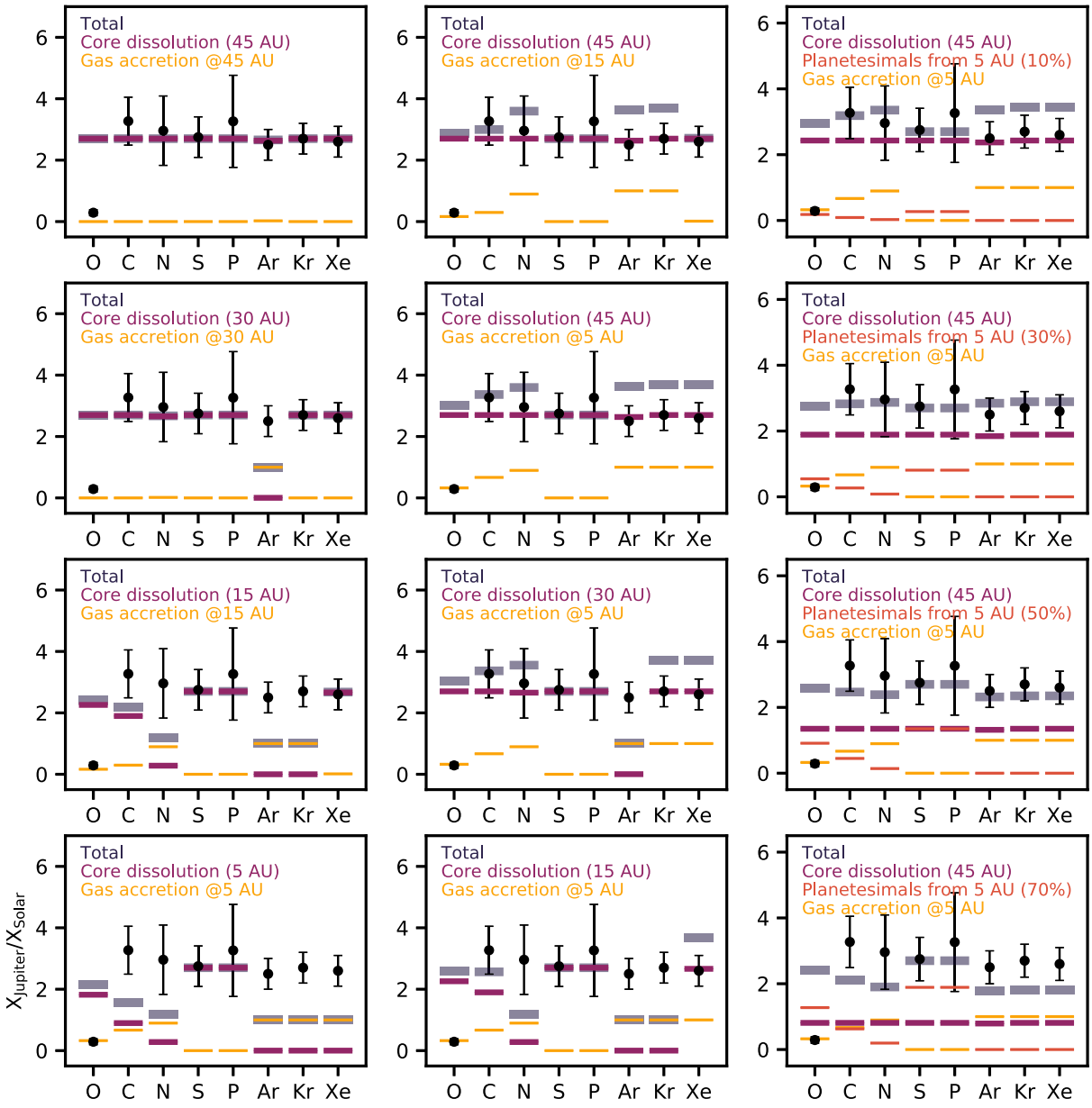

Figure 4. Same as Figure 3, but for different combinations of solid and gas accretion locations. Left: predicted elemental enhancements in Jupiter's envelope when solids and envelope are accreted at the same disk radius. Middle: predicted elemental enhancements when the gas is accreted interior to the core formation location. Right: predicted enhancements when a fraction of the solids dissolved in the enveloped originates from a core formed at 45 au and a fraction from planetesimals accreted at 5 au. Note that only scenarios where Jupiter's core forms at 45 au fit all data. If Ar condenses out closer to the N_2 snowline, as suggested by recent unpublished data, core formation beyond 30 au is sufficient to explain observations.

ORCID iDs

Karin I Öberg https://orcid.org/0000-0001-8798-1347